New Rules for AAAS–Newcomb Cleveland Prize

The AAAS–Newcomb Cleveland Prize, which previously honored research papers presented at AAAS annual meetings, will henceforth be awarded annually to the author of an outstanding paper published from September through August in the Reports section of *Science*. The first competition year under the new rules starts with the 3 September 1976 issue of *Science* and ends with that of 26 August 1977. The value of the prize has been raised from $2000 to $5000; the winner also receives a bronze medal.

To be eligible, a paper must be a first-time presentation (other than to a departmental seminar or colloquium) of previously unpublished results of the author's own research. Reference to pertinent earlier work by the author may be included to give perspective.

Throughout the year, readers are invited to nominate papers appearing in the Reports section. Nominations must be typed, and the following information provided: the title of the paper, issue in which it is published, author's name, and a brief statement of justification for nomination. Nominations should be submitted to the AAAS–Newcomb Cleveland Prize, AAAS, 1515 Massachusetts Avenue, NW, Washington, D.C. 20005. Final selection will rest with a panel of scientists appointed by the Board of Directors.

The award will be presented at a session of the annual meeting at which the winner will be invited to present a scientific paper reviewing the field related to the prize-winning research. The review paper will subsequently be published in *Science*. In cases of multiple authorship, the prize will be divided equally between or among the authors; the senior author will be invited to speak at the annual meeting.

Reports

Visual Observations of the Sea Floor Subduction Line in the Middle-America Trench

Abstract. *Four dives were made to the floor of the Middle-America Trench with the U.S. Navy's deep research submersible DSV* Turtle. *The area investigated is located between Costa Rica and the Cocos Ridge where the depth of the trench floor does not exceed the 2000-meter capability of the submersible. At the axis of the trench floor a series of steep northeast-facing scarps 10 to 20 meters high lie parallel to the trench axis. Here oceanic crust appears to have been carried down by near-vertical normal vaults of small displacement. Between these small scarps and the landward wall of the trench a narrow line of recent deformation interrupts a smooth apron. Unconsolidated sediments are thrust in sharply serrated piles and cut by sharp-edged chasms. This line of deformation is interpreted as the present sea floor trace of crustal subduction.*

Remarkably, the compelling array of evidence cited in support of contemporary subduction has not included visual field observations at the proposed sites of subduction (*1*). The observation that Benioff earthquake planes intersect the seabed somewhere in the trenches (*2*) implies that differential motion must extend to the sea floor and should have visible manifestations on the seabed (*3*). Although somewhere on or near the landward wall seems a probable site, the present accuracy of hypocentral determination is insufficient to define the exact location of the seabed trace of subduction.

The accumulation in trenches of undeformed stratified sediments (*4*) has been cited as evidence against presently active motion related to subduction (*5*), but in fact, the resolution of presently available high-precision echo sounders and seismic profilers is not sufficient to resolve potentially different structural patterns near precipitous slopes at such great depths.

Subduction now plays an immensely important role in modern tectonic schemes; yet the subject retains a misty character, since all details are inferred from indirect geophysical measurements (*6*) or are geological reconstructions based on complex superimposed records retained in deformed ancient rocks. The visual study of a suspected contemporary subduction zone reported here was initiated in order to gain a better understanding of the initial phases of subduction, particularly in regard to the role and fate of deep-sea sediments.

During April 1975 we made four dives in DSV *Turtle* to the floor of the Middle-America Trench (*7*). Three dives (32, 33, and 35) revealed a consistent pattern of deformation. On the fourth dive (34) a seamount embedded in the landward wall of the trench (Fig. 1) was examined. The 1975 diving program also included 14 dives on the Cocos Ridge (*8*). On that series, evidence of active faulting and uplift was observed on the northern Cocos Ridge southeast of the trench area described in this report.

A series of northeast-facing scarps lie at the trench axis. Nearly identical morphology and surface characteristics were observed on the scarps during each of the five traverses [dives 32 (1), 33 (2), 35 (2)] of these cuesta-like features. The (60° to 80°) scarps are 10 to 30 m high and approximately 150 m apart (Fig. 2). Along the crest of each ridge, broken angular blocks of unconsolidated sediments litter the sea floor. Outcrops of dense, gray, fine-grained limestone occur a few meters below the crest of each ridge. The outcropping rocks were devoid of the manganese coatings usually seen on deep-sea exposures. The limestone (three samples, dive 33) contains a few mineral grains presumably derived from penecontemporaneous volcanic exposures. A weak current supports scattered populations of sponges and sea fans which attach themselves to outcropping rocks. The narrow sediment ramps which lap on the base of each scrap are smooth and undisturbed. It is concluded that the small cuestas represent a series of recently active but currently inactive normal faults of small displacement which have downfaulted the oceanic crust and its pelagic cover.

Throughout the four dives reported here the quantity of large organic particulate matter in the water column was high as compared to that in the clear waters encountered further seaward on the Cocos Ridge (*8*). The particulate concentrations which result from the relatively high surface productivity of the area must result in higher deposition rates in the trench area than would occur further seaward. Strong backscatter of light from the particulate matter impaired the quality of the photographs (Fig. 3).

A gently sloping, tranquil, ooze-covered bottom extends for about 200 m from the base of the northeasternmost cuesta scarp of the trench axis to the foot of the landward wall of the trench (Fig. 2). With the notable exception of a dramatic deformed zone (Figs. 3 and 4) which longitudinally bisects the apron, this portion of the trench floor is otherwise devoid of surface expressions of deformation.

Contemporary deformation is creating sharp, serrated shapes and strikingly angular blocks in the unconsolidated green silty ooze of the trench floor (Fig. 3). The deformation has broken the unconsolidated sediment and uplifted blocks 1 to 3 m above the surface of the apron. It has pulled sediment apart, forming long (> 30 m), narrow (1 to 3 m wide), bifurcating chasms which form an uneven line parallel to the trench axis. Remarkably, this contemporary deformation is limited to an extremely narrow belt less than 30 m in width. The most recent deformation occurred not long before our visit. Although animals were burrowing new holes into the recently exposed sediment slopes, neither the benthic fauna nor the currents had yet appreciably altered the shapes of the sharpest uplifted forms. Apparently the fissures which appeared slightly rounded and partly filled were a little older. But all signs of deformation on the apron, both strictly contemporary and slightly older, were limited to this one narrow zone.

An abrupt but even and uneventful change in slope marks the boundary between the smooth gently sloping apron of the trench floor and the equally smooth but precipitous, sediment-covered trench wall (Fig. 2). We observed absolutely no signs of deformation at or near the base of the wall during any of the three traverses (see Fig. 1 for locations). Thus, this major morphological boundary which is frequently taken as the structural boundary between continental and oceanic crust is not associated with any visually observable active surface manifestations of contemporary deformation. The landward trench wall is extremely complex and varied. Much of it is a steep, smooth, sediment-covered slope, but locally on smaller (~ 30 m) escarpments sharp-edged, V-shaped grooves 0.5 to 2 m deep and 1 to 2 m wide cut a geometrical pattern almost precisely up and down slope, often becoming somewhat mantled by sediments before completely disappearing. The V-shaped grooves expose bedding and parting planes in the essentially unconsolidated sediments. Here and there, shells, pebbles, and rubble were seen in and near the downslope ends of the regularly spaced V-shaped notches.

Several narrow, nearly level, benches on the wall revealed outcrops of bedrock and scattered rubble. In marked contrast to the almost barren sediment-covered wall, the filter feeders attached to nearly every boulder or outcrop lend a garden-like aspect to the rocky benches.

Less than 1 km east of the site of dive 32, the axis of the Middle-America Trench passes over a shallow saddle of 1600 m. Southeast of the saddle, sediments ponded between the trench wall and the Cocos Ridge crest have created a small abyssal plain which abuts the trench wall. As we began dive 34 at the northern edge of the plain, we antici-

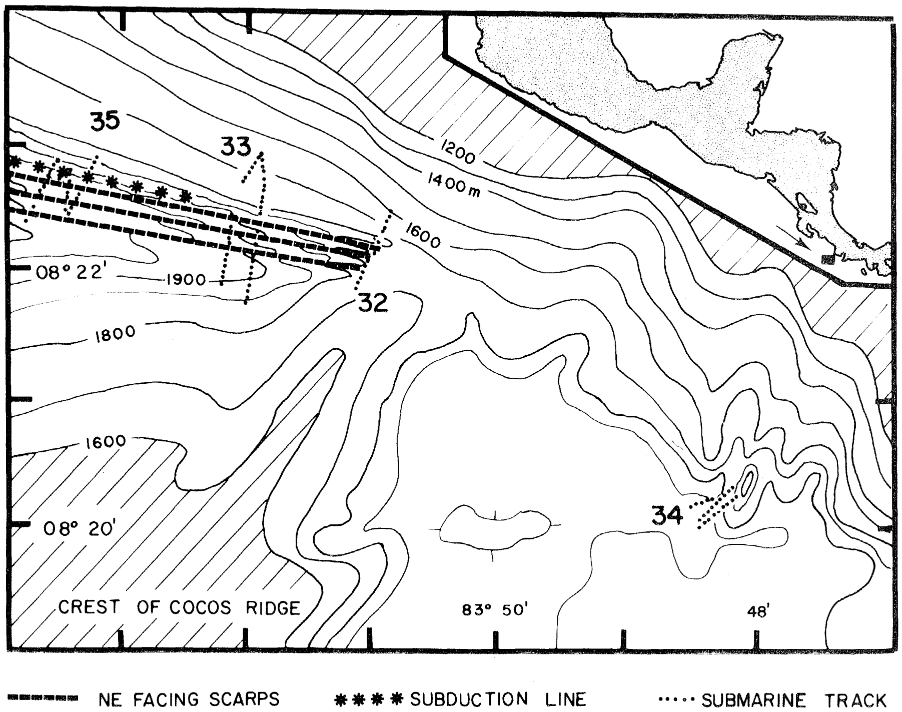

Fig. 1. Southeast Middle-America Trench with locations of DSV *Turtle* dives 32, 33, 34, and 35, April 1975. Isobaths (meters) in the vicinity of the dives are based on echo-sounding profiles (Precision depth recorder) obtained by M.V. *Maxine D* during dive site survey in April 1975.

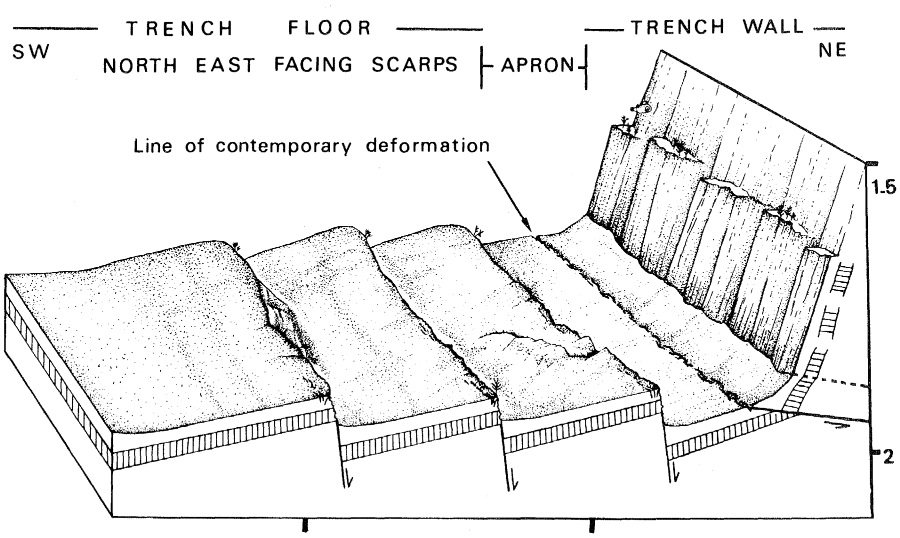

Fig. 2. Visual observations and structural inferences (natural scale), southeast Middle-America Trench. Visual observations were made on DSV *Turtle* dives 32, 33, and 35 (see Fig. 1 for geographical location of each dive). Northeast-facing scarps of trench floor are interpreted as normal faults which have carried oceanic crust down along trench axis. Smooth trench floor apron is bisected by zone of contemporary deformation which is interpreted as the sea floor trace of subduction (see Figs. 3 and 4). The landward wall is to the right.

pated that contemporary deformation might be recognized in the ponded sediments of the plain, but this was not the case. The plain sharply abutted the landward slope without any signs of deformation. At the dive site, the steep slope encountered ran northeast-southwest at approximately right angles to the regional strike of the trench wall. This slope is composed of undeformed lava pillows and lava cylinders. The scene was identical to depositional lava terrain which we have repeatedly observed on seamounts (*8, 9*). This seamount now embedded in the trench wall has not yet undergone significant deformation. It seems to have just reached the subduction zone.

The northeast-facing scarps of the trench axis are interpreted as normal faults which have carried down the oceanic crust and its pelagic cover (Fig. 2). Seismic reflection profiles reveal that elsewhere normal faults of much larger displacement form the seaward wall of the trench (*7*). The zone of deformation within the trench apron apparently marks the sea floor trace of active subduction. Our observations show that at the present time no movement is occurring at the base of the landward wall and that probably no significant deformation has occurred there for decades or centuries. On this wall, benches with outcropping rocks mark structural breaks. The geometrical pattern of V-shaped grooves oriented up and down slope entirely without bifurcation suggests a structural rather than erosional origin, although it is clear that slides and rock falls have recently occurred along many of these strange V grooves. The trench wall was far too varied along the four traverses [dive 32 (1), dive 33 (2), and dive 35 (1)] to discern a general pattern. Perhaps the most surprising observation was that most of the steep wall is covered by smooth undisturbed ooze.

At the sites of dives 32, 33, and 35, the trench plunges northwest at a gradient of 1 : 15, which would preclude any sediments from ponding along the trench axis. Any turbidites would be transported 500 km to the northwest into the deepening trench. Thus the behavior and pattern of deformation observed here should differ from the deeper parts of the trench in that the trench floor turbidites will be absent from the apron and landward wall sequence. We observed no features which could be attributed to turbidite erosion or deposition. The moderate currents (< 15 cm/sec) left no scour or depositional forms in the almost pure pelagic depositional environment. This tranquility greatly enhanced the visual contrast between the undeformed and the deformed sea floor.

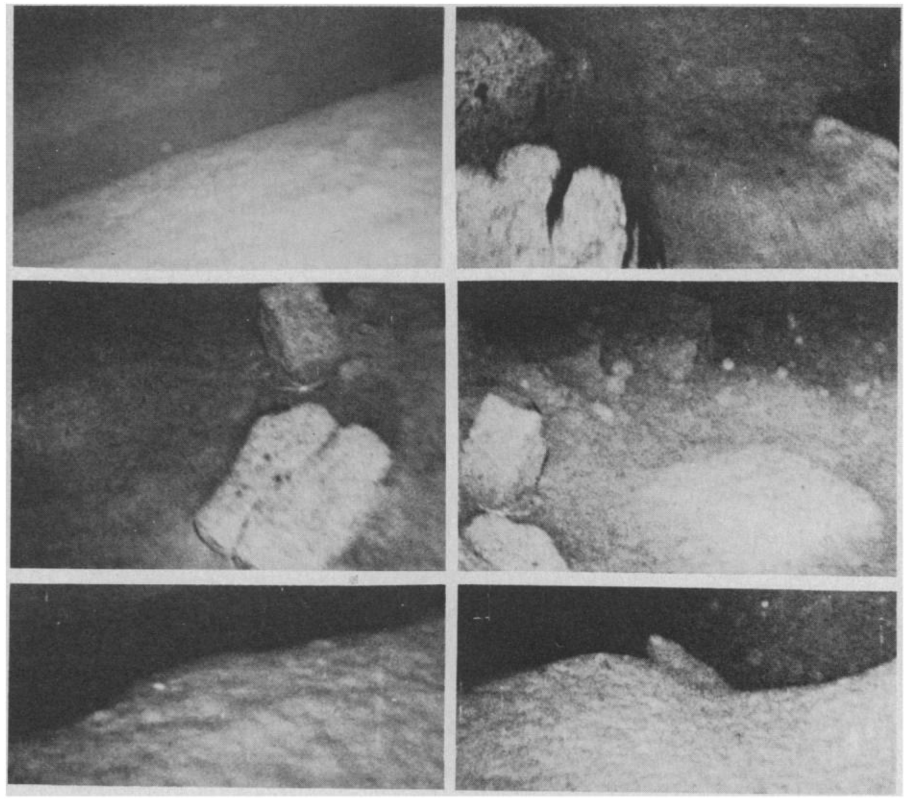

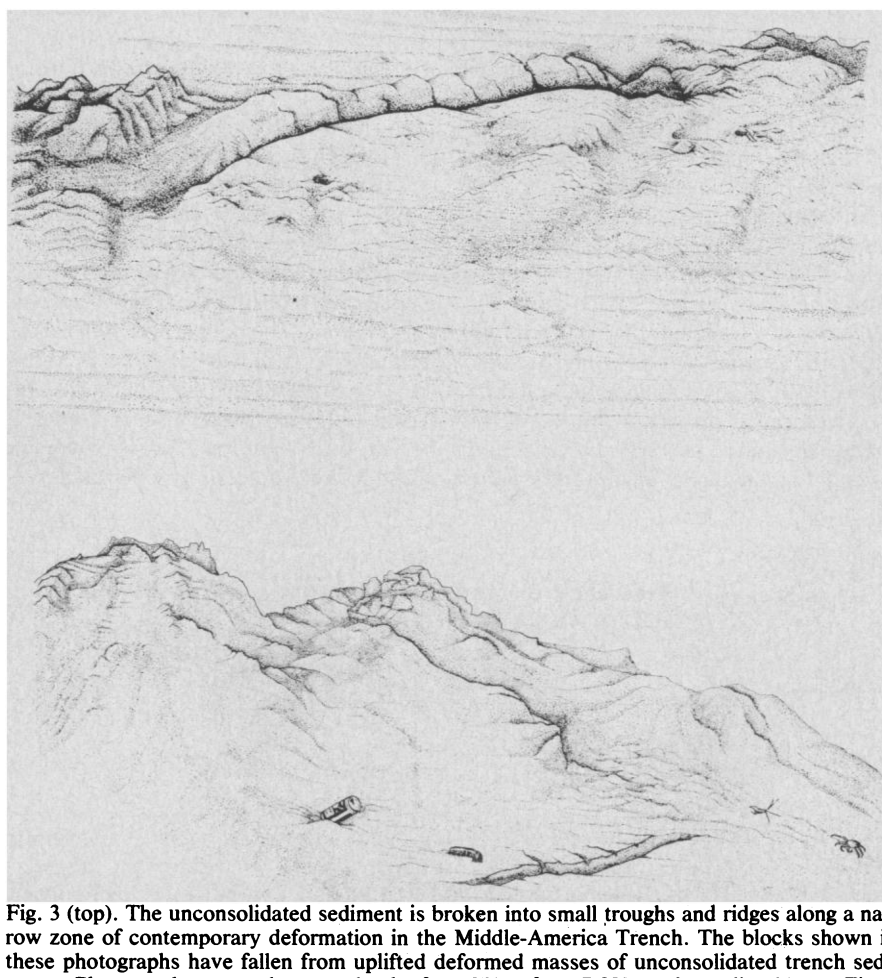

Fig. 3 (top). The unconsolidated sediment is broken into small troughs and ridges along a narrow zone of contemporary deformation in the Middle-America Trench. The blocks shown in these photographs have fallen from uplifted deformed masses of unconsolidated trench sediments. Photographs were taken at a depth of ~ 1875 m from DSV *Turtle* on dive 35. Fig. 4 (bottom). Scenes looking northwest across the narrow zone of contemporary deformation in the floor of the Middle-America Trench which may mark the sea floor manifestation of the subduction plane (Fig. 2). The upper scene is 30 m wide. A bifurcated chasm is in unconsolidated silty ooze. The lower scene is 2 m wide. Sharp crests of angular blocks of silty unconsolidated ooze are uplifted a few meters above the trench floor.

One serious limitation of the present study was the lack of precision navigation for either the submersible or the surface ship and the lack of subbottom profiler records precisely located with respect to the submersible traverses.

BRUCE C. HEEZEN
MICHAEL RAWSON

Lamont-Doherty Geological Observatory of Columbia University, Palisades, New York 10964

References and Notes

1. The Mariana Trench, a recognized subduction zone, was the site of the first descent by man to the ocean's greatest depths [J. Piccard and R. S. Dietz, *Seven Miles Down* (Putnam, New York, 1961)]. The Puerto Rico and Japan trenches were later explored with the bathyscaphe *Archimède* [G. Bellaiche, *C. R. Acad. Sci.* **265**, 1160 (1967); J. M. Peres, *Deep-Sea Res.* **12**, 883 (1965)]. These observers noted fresh unstable talus slopes as evidence of contemporary deformation. However, they did not relate their observations either to the then rather novel subduction process or to older structural models.
2. P. Molnar and L. R. Sykes, *Bull. Geol. Soc. Am.* **80**, 1639 (1969).
3. D. E. Karig and G. F. Sharman, *ibid.* **86**, 377 (1976).
4. W. J. Ludwig, J. Ewing, M. Ewing, S. Murauchi, N. Den, S. Asano, H. Hotta, M. Hayakawa, T. Asanuma, K. Ichikawa, I. Noguchi, *J. Geophys. Res.* **71**, 2121 (1966); J. Ewing and M. Ewing, *ibid.* **67**, 4729 (1962).
5. D. W. Scholl, R. Von Huene, J. B. Ridlon, *Science* **159**, 869 (1968).
6. D. R. Seely, P. R. Vail, G. G. Walton, in *The Geology of Continental Margins*, C. A. Burk and C. L. Drake, Eds. (Springer-Verlag. New York, 1974), pp. 249–260.
7. R. L. Fisher, *Bull. Geol. Soc. Am.* **72**, 703 (1961).
8. B. C. Heezen and M. Rawson, *Mar. Geol.* **23**, 173 (1977).
9. D. J. Fornari, A. Malahoff, B. C. Heezen, *Bull. Geol. Soc. Am.*, in press.
10. This research is supported by the U.S. Navy Office of Naval Research under contract N00014-76-C-0264. We gratefully acknowledge the cooperation of the officers and men of DSV *Turtle* and others of the U.S. Navy Submarine Development Group One. The illustrations were done by Suzanne MacDonald. Lamont-Doherty Geological Observatory Contribution 2488.

24 September 1976; revised 17 December 1976

Laser Interferometer Measurement of Changes in Crayfish Axon Diameter Concurrent with Action Potential

Abstract. *Small rapid changes in the diameter of an axon take place when an action potential progresses along the axon. In the giant axon of the crayfish these occur within a period of about 1 millisecond and are typically about 18 angstroms in total amplitude.*

Previous studies have shown that there are slow mechanical changes in nervous tissue in conjunction with an action potential (*1–4*). We have observed that when an action potential travels along an axon, the outer surface of the axon undergoes a displacement time pattern that transpires within a few milliseconds. These motions are fundamentally different from those previously observed in single cells during the course of an action potential in the algae *Nitella* and *Chara* (*2, 4*). Such motions occur over periods of seconds rather than milliseconds.

We used a laser interferometer to measure axon boundary movement accompanying the action potential in the medial giant axon of the crayfish *Procambarus clarkii*. The optical layout of the interferometer is shown in Fig. 1a. It is similar to that described by Eberhardt and Andrews (*5*), but it has a special optic fiber in the target path and features a phase-locked detection scheme developed at Stanford (*6*) which has a sensitivity only 6 db lower than that of a homodyne system and is simpler than FM detection for measurement of transients.

The optic fiber is a graded-index fiber wave guide manufactured by Corning Glass Works. It consists of a core about 80 μm in diameter surrounded by another layer of glass, bringing the total diameter of the fiber to approximately 150 μm. Its useful property for our purpose is that the core, which carries most of the light, preserves the spatial coherence of the light because its index of refraction decreases approximately parabolically with increasing radius (*7*).

Light from the target is reflected through the optic fiber back into the photodetector, where it is mixed with light from the reference beam that has been downshifted in frequency by 40 Mhz at the Bragg cell. If the target motion is given by $x(t)$, the phase shift in the returning beam is given by

$$\phi(t) = \frac{4\pi n x(t)}{\lambda}$$

where λ is the wavelength of He-Ne light (6328 Å) and n is the index of refraction of the target medium (1.33 for water). The current from the square-law photodetector contains a component at the difference frequency of the two beams (*8*)

$$i \sim \cos[2\pi f t + \phi(t) + \phi_0]$$

where f is the "carrier" frequency (40 Mhz) and ϕ_0 is the quasi-static phase due to the path length difference between the target and the reference.

To detect the phase modulation $\phi(t)$, the signal is converted to a 100-khz carrier and then multiplied by a reference sinusoid that is 90° out of phase with the

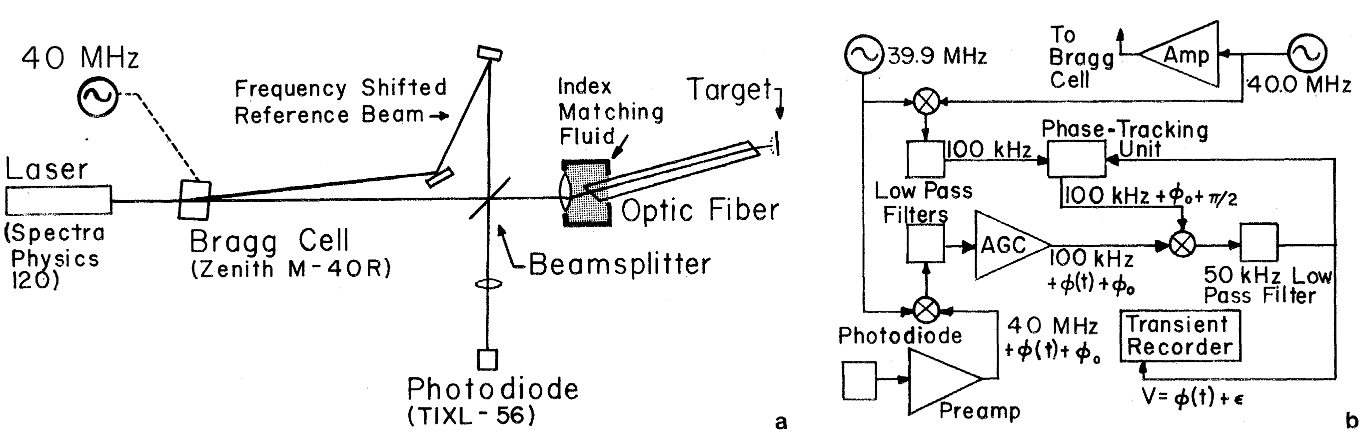

Fig. 1. Interferometer measuring system. (a) Optical system: the Bragg cell is an acousto-optic modulator, which shifts the frequency of part of the incoming light by 40 Mhz and deflects it away from the unshifted (target) beam. The photodetector is an avalanche photodiode. (b) Signal detection system: the phases of the signal and reference sinusoid are indicated at various stages of processing. The 40-Mhz carrier is converted to 100 khz so that the digital phase shifter in the phase-tracking unit need not perform at radio frequency. The automatic gain control (*AGC*) maintains the carrier at an amplitude of 10 volts to the final multiplier, so the detected phase modulation will not vary with shifts in carrier level from the photodetector. The detected output contains a d-c term ϵ, which appears if the reference sinusoid to the final multiplier shifts away from quadrature with the carrier; this voltage functions as an error signal to the feedback system.